

The GW signal from primordial magnetic fields in the PTA frequency band

12th Iberian Gravitational Waves Meeting
Jun. 8, 2022



Alberto Roper Pol
Postdoctoral Researcher

Laboratoire Astroparticule et Cosmologie (APC)
Université de Paris, CNRS



Collaborators: A. Brandenburg (Nordita), **C. Caprini (APC)**, T. Kahniashvili (CMU), A. Kosowsky (PittU), S. Mandal (SBU), **A. Neronov (APC)**, **D. Semikoz (APC)**.

ARP, C. Caprini, A. Neronov, D. Semikoz, *Phys. Rev. D* **105**, 123502 (2022), arXiv:2201.05630

A. Neronov, ARP, C. Caprini, D. Semikoz, *Phys. Rev. D* **103**, L041302 (2021), arXiv:2009.14174

ARP et al., *Phys. Rev. D* **102**, 083512 (2020), arXiv:1903.08585

ARP et al., *JCAP* **04** (2022), 019, arXiv:2107.05356 (2021)

https://github.com/AlbertoRoper/GW_turbulence

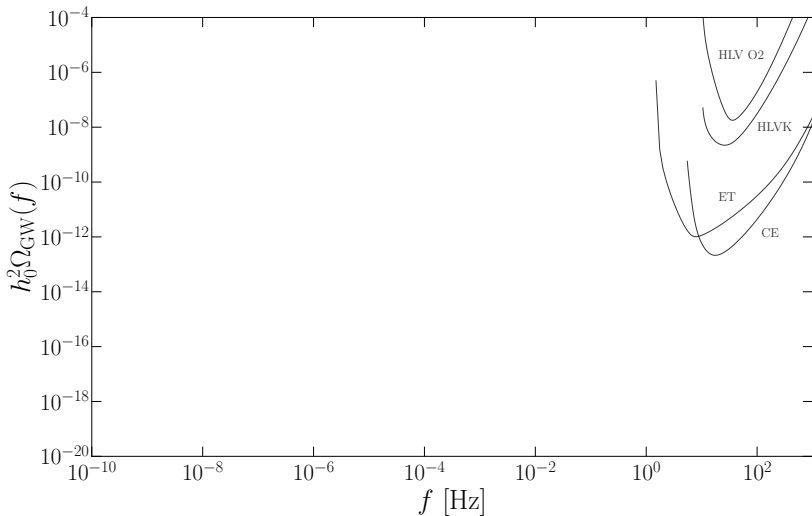
Probing the early Universe with GWs: Cosmological GW background

- Why background? Individual sources are not resolvable, superposition of single events occurring in the whole Universe
- From phase transitions
 - Ground-based detectors (LVK, ET, CE) frequencies are 10–1000 Hz [see **A. Romero-Rodríguez talk**]
Peccei-Quinn, B-L, left-right symmetries, ... $\sim 10^7, 10^8$ GeV (untested physics, SM extensions)
 - Space-based detectors (LISA) frequencies are 10^{-5} – 10^{-2} Hz
Electroweak phase transition ~ 100 GeV ($f_c \sim 10^{-5}$ Hz)
 - Pulsar Timing Array (**PTA**) frequencies are 10^{-9} – 10^{-7} Hz
Quantum chromodynamic (QCD) phase transition
 ~ 100 MeV ($f_c \sim 10^{-9}$ Hz)
- From inflation
 - *B*-modes of CMB anisotropies ($f_c \sim 10^{-18}$ Hz)
 - Can cover all *f* spectrum, depending on end-of-reheating *T*, and blue-tilted (beyond slow-roll inflation)

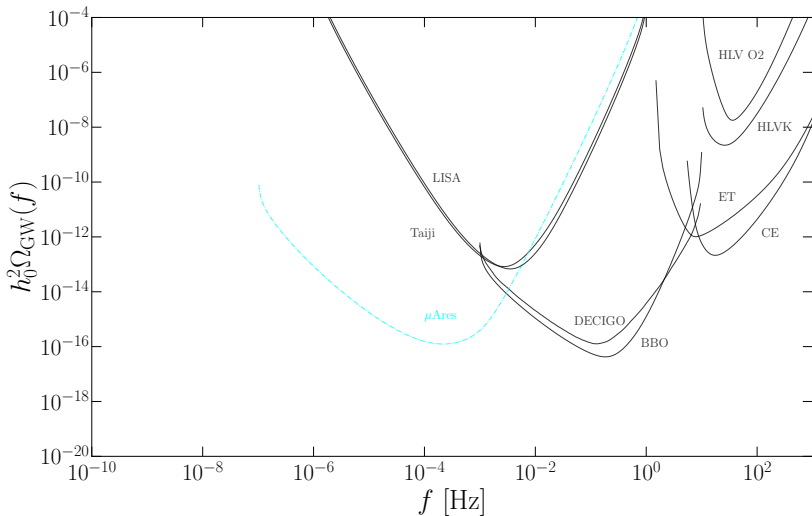
MHD sources in the early universe

- Magnetohydrodynamic (MHD) sources of GWs
 - Hydrodynamic turbulence from first-order phase transitions
 - **Primordial magnetic fields**
- High-conductivity of the early universe leads to a high-coupling between magnetic and velocity fields
- Other sources of GWs include
 - True vacuum bubble collisions
 - Sound waves [see **D. Weir** talk]
 - Cosmic topological defects (cosmic strings)
 - Primordial black holes [see **J. García-Bellido** talk]

Gravitational spectrum (ground-based detectors)



Gravitational spectrum (space-based detectors)



Pulsar Timing Array (PTA) collaborations

- An array of pulsars is observed to compute the delays on the time of arrival due to the presence of GWs
- International collaborations (IPTA)
 - European Pulsar Timing Array (EPTA)
 - North American Nano-Hertz Observatory for Gravitational Waves (NANOGrav)
 - Parkes Pulsar Timing Array (PPTA)
 - Indian Pulsar Timing Array Project (InPTA)

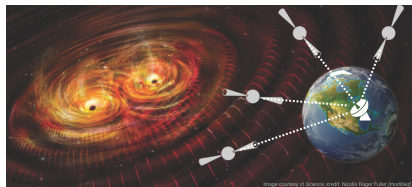
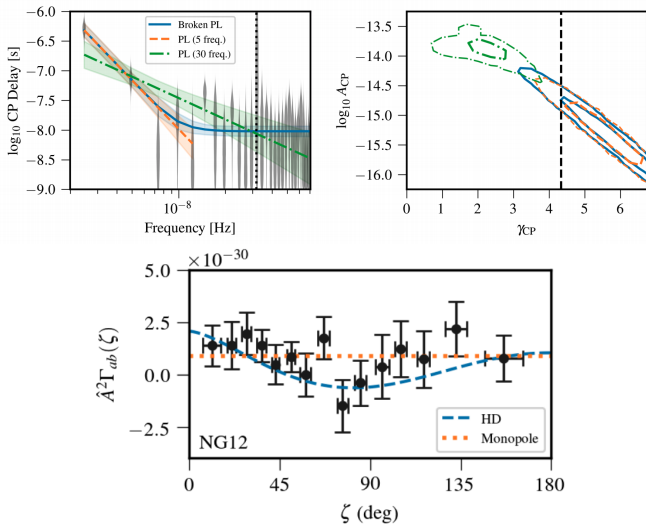


Figure: Image courtesy of Science, credit: Nicolle Rager Fuller

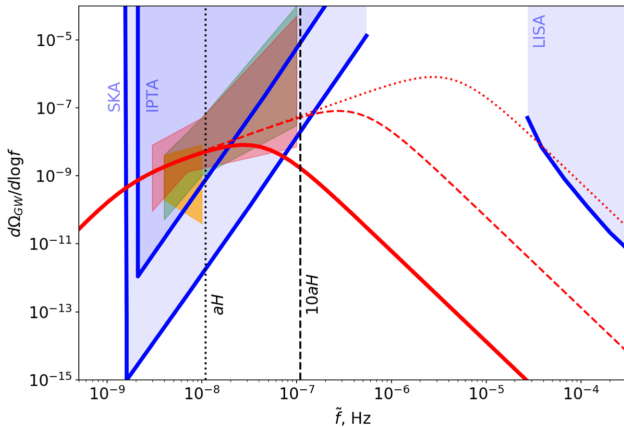


NANOGrav 12.5 yr data observation¹



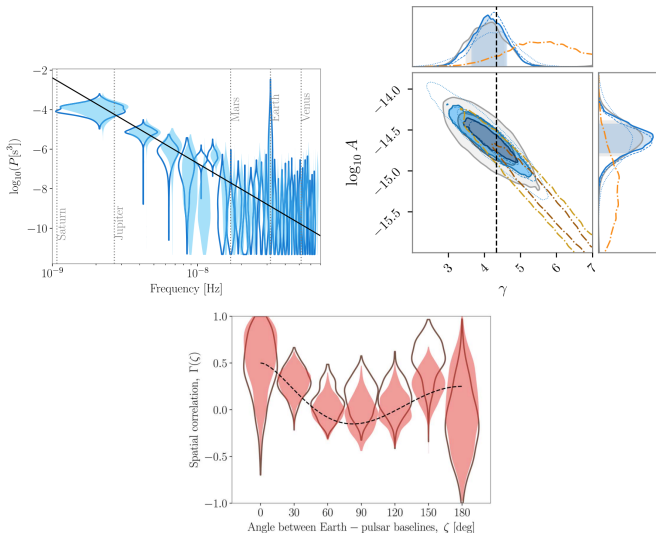
¹[NANOGrav collaboration], *ApJ Lett.* **905**, 2 (2020)

Detectability of the SGWB produced by non-helical
primordial magnetic fields from the QCD phase transition
by NANOGrav²

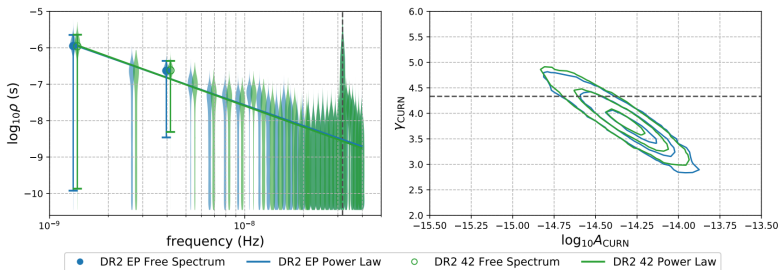


²A. Neronov, ARP, C. Caprini and D. Semikoz,
Phys. Rev. D **103**, L041302 (2021)

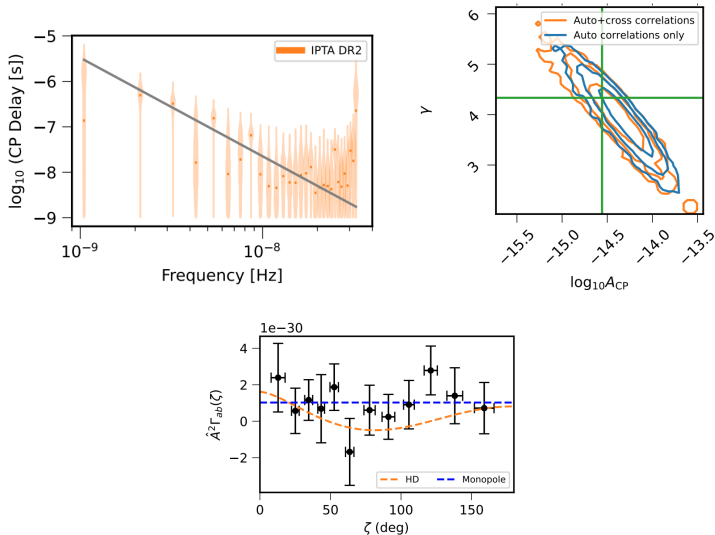
PPTA 15 yr data observation³



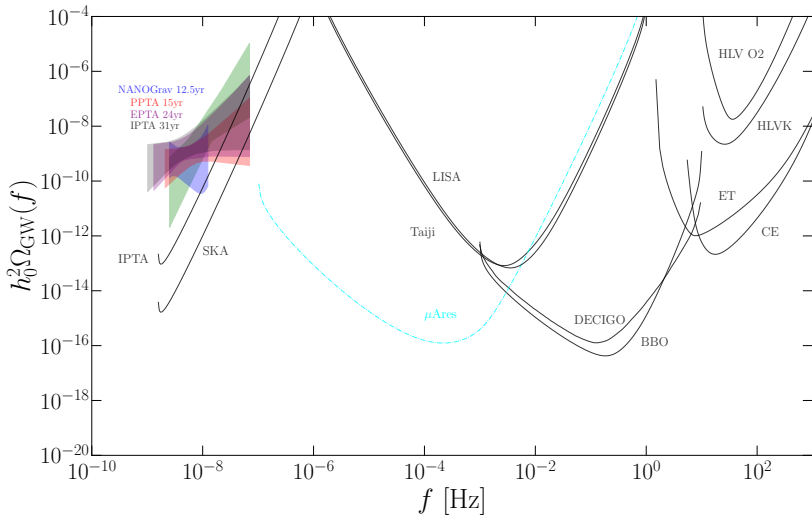
EPTA 24 yr data observation (DR 2)⁴



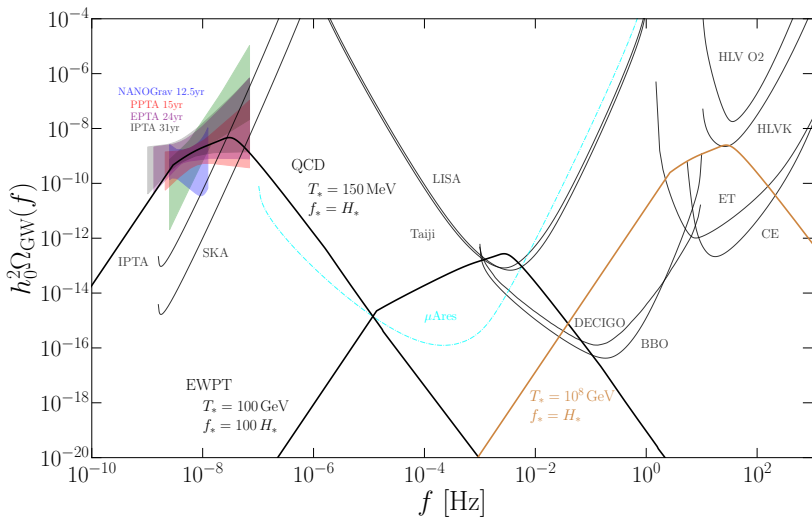
IPTA combined data observation (DR 2)⁵



Gravitational spectrum (PTAs)



Gravitational spectrum (PTAs)⁶



⁶ ARP, C. Caprini, A. Neronov, D. Semikoz,
Phys. Rev. D **105**, 123502 (2022)

How do we compute these signals?

- Direct numerical simulations using the `PENCIL CODE`⁷ to solve:
 - Relativistic MHD equations adapted for radiation-dominated era (after electroweak symmetry is broken)
 - Gravitational waves equation
- Numerical simulations are necessary to solve MHD dynamics and to take into account the exact unequal time correlator of the GW sourcing term (analytical estimates require simplifying assumptions).
- The assumption that the two-point correlations of the magnetic stress are constant in time accurately explains the numerical results when the eddy-turnover time is large (slow turbulent evolution) for initially present nonhelical fields⁸.

⁷ Pencil Code Collaboration, *JOSS* **6**, 2807 (2020), <https://github.com/pencil-code/>

⁸ ARP, C. Caprini, A. Neronov, D. Semikoz,
Phys. Rev. D **105**, 123502 (2022)

MHD description

Right after the electroweak phase transition we can model the plasma using continuum MHD

- Charge-neutral, electrically conducting fluid
- Relativistic magnetohydrodynamic (MHD) equations
- Radiation-dominated Universe

$$p = \rho c^2/3,$$

i.e. $w = 1/3$ (ultrarelativistic EoS)

- Friedmann–Lemaître–Robertson–Walker metric

$$g_{\mu\nu} = \text{diag}\{-1, a^2, a^2, a^2\}$$

Contributions to the stress-energy tensor

$$T^{\mu\nu} = \left(\frac{p}{c^2} + \rho\right) U^\mu U^\nu + p g^{\mu\nu} + \pi^{\mu\nu} + F^{\mu\gamma} F^\nu{}_\gamma - \frac{1}{4} g^{\mu\nu} F_{\lambda\gamma} F^{\lambda\gamma},$$

- From fluid motions

$$T_{ij} = \left(\frac{p}{c^2} + \rho\right) \gamma^2 u_i u_j + p \delta_{ij}$$

- Ultrarelativistic EoS:

$$p = \rho c^2 / 3$$

- Viscous stresses:

$$\pi_{ij} = 2\nu(p/c^2 + \rho) S_{ij}$$

- 4-velocity $U^\mu = \gamma(c, u^i)$
- 4-potential $A^\mu = (\phi/c, A^i)$

- From magnetic fields:

$$T_{ij} = -B_i B_j + \delta_{ij} B^2 / 2$$

- 4-current $J^\mu = (c\rho_e, J^i)$
- Faraday tensor
 $F^{\mu\nu} = \partial^\mu A^\nu - \partial^\nu A^\mu$

Conservation laws

$$T^{\mu\nu}{}_{;\nu} = 0$$

We assume subrelativistic motions:

$$\gamma^2 \sim 1 + (v/c)^2 + \mathcal{O}(v/c)^4$$

Relativistic MHD equations are reduced to⁹

$$\frac{\partial \ln \rho}{\partial t} = -\frac{4}{3} (\nabla \cdot \mathbf{u} + \mathbf{u} \cdot \nabla \ln \rho) + \frac{1}{\rho} [\mathbf{u} \cdot (\mathbf{J} \times \mathbf{B}) + \eta J^2],$$

$$\begin{aligned} \frac{D\mathbf{u}}{Dt} &= \frac{1}{3} \mathbf{u} (\nabla \cdot \mathbf{u} + \mathbf{u} \cdot \nabla \ln \rho) - \frac{\mathbf{u}}{\rho} [\mathbf{u} \cdot (\mathbf{J} \times \mathbf{B}) + \eta J^2] \\ &\quad - \frac{1}{4} \nabla \ln \rho + \frac{3}{4\rho} \mathbf{J} \times \mathbf{B} + \frac{2}{\rho} \nabla \cdot (\rho \nu \mathbf{S}) + \mathcal{F}, \end{aligned}$$

$$\frac{\partial \mathbf{B}}{\partial t} = \nabla \times (\mathbf{u} \times \mathbf{B} - \eta \mathbf{J} + \mathcal{E}), \quad \mathbf{J} = \nabla \times \mathbf{B},$$

for a flat expanding universe with comoving and normalized

$\rho = a^4 \rho_{\text{phys}}$, $\rho = a^4 \rho_{\text{phys}}$, $B_i = a^2 B_{i,\text{phys}}$, u_i , and conformal time t ($dt = a dt_c$).

⁹A. Brandenburg, et al., *Phys. Rev. D* **54**, 1291 (1996)

GWs equation for an expanding flat Universe

- Assumptions: isotropic and homogeneous Universe
- Friedmann–Lemaître–Robertson–Walker (FLRW) metric $\gamma_{ij} = a^2 \delta_{ij}$
- Tensor-mode perturbations above the FLRW model:

$$g_{ij} = a^2 \left(\delta_{ij} + h_{ij}^{\text{phys}} \right), \quad |h_{ij}^{\text{phys}}| \ll |g_{ij}|$$

- GW equation is¹⁰

$$\left(\partial_t^2 - \frac{a''}{a} - c^2 \nabla^2 \right) h_{ij} = \frac{16\pi G}{ac^2} (T_{ij}^{\text{TT}} + \cancel{t_{ij}})$$

- h_{ij} are rescaled $h_{ij} = ah_{ij}^{\text{phys}}$
- Comoving spatial coordinates $\nabla = a\nabla^{\text{phys}}$
- Conformal time $dt = a dt_c$
- Comoving stress-energy tensor components $T_{ij} = a^4 T_{ij}^{\text{phys}}$
- Radiation-dominated epoch such that $a'' = 0$
- Nonlinear leading-order term $t_{ij} \propto \partial_i h_{lm}^{\text{TT}} \partial_j h_{lm}^{\text{TT}}$ omitted¹¹

¹⁰L. P. Grishchuk, *Sov. Phys. JETP* **40**, 409 (1974)

¹¹Y. He, ARP and A. Brandenburg, *submitted to Phys. Rev. D*, arXiv:2110.14456 (2021)

Numerical results for decaying MHD turbulence¹²

Initial conditions

- Initial stochastic non-helical magnetic field
- Batchelor spectrum, i.e., $E_M \propto k^4$ for small $k < k_*$
- Kolmogorov spectrum in the inertial range, i.e., $E_M \propto k^{-5/3}$

$$kB_i = \left(\delta_{ij} - \hat{k}_i \hat{k}_j \right) g_j \sqrt{2E_M(k)},$$
$$E_M(k) = E_M^* \left(\frac{17}{5} \right)^{1/\alpha} \frac{(k/k_*)^4}{\left[1 + \frac{12}{5} (k/k_*)^{\alpha(4+5/3)} \right]^{1/\alpha}}; \quad \alpha = 2$$

¹²A. Brandenburg *et al.*, *Phys. Rev. D* **96**, 123528 (2017)

ARP *et al.*, *Phys. Rev. D* **102**, 083512 (2020)

ARP *et al.*, *JCAP* **04** (2022), 019

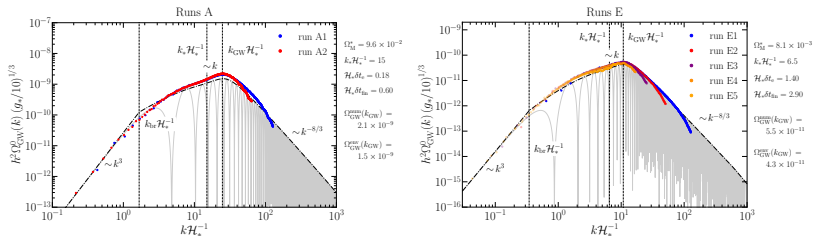
ARP *et al.*, *Phys. Rev. D* **105**, 123502 (2022)

Numerical results for decaying MHD turbulence

Free parameters on the initial conditions

- Magnetic energy density at t_* is a fraction of the radiation energy density, $\Omega_M = \mathcal{E}_M / \mathcal{E}_{\text{rad}}^* = \frac{1}{2} B_0^2 \leq 0.1$ (BBN limit).
- Spectral peak k_* , normalized by H_*/c , is given by the characteristic scale of the sourcing turbulence (as a fraction of the Hubble radius) and should be $k_* \geq 2\pi$ by causality.
- Time t_* at which the magnetic field is generated, corresponding to the temperature scale T_* (e.g., $T_* \sim 150$ MeV at the QCD phase transition).

Numerical results for decaying MHD turbulence¹³



run	Ω_M^*	$k_* \mathcal{H}_*^{-1}$	$\mathcal{H}_* \delta t_e$	$\mathcal{H}_* \delta t_m$	$\Omega_{\text{GW}}^{\text{num}}(k_{\text{GW}})$	$[\Omega_{\text{GW}}^{\text{env}}/\Omega_{\text{GW}}^{\text{num}}](k_{\text{GW}})$	n	$\mathcal{H}_* L$	$\mathcal{H}_* t_{\text{end}}$	$\mathcal{H}_* \eta$
A1	9.6×10^{-2}	15	0.176	0.60	2.1×10^{-9}	1.357	768	6π	9	10^{-7}
A2	—	—	—	—	—	—	768	12π	9	10^{-6}
E1	8.1×10^{-3}	6.5	1.398	2.90	5.5×10^{-11}	1.184	512	4π	8	10^{-7}
E2	—	—	—	—	—	—	512	10π	18	10^{-7}
E3	—	—	—	—	—	—	512	20π	61	10^{-7}
E4	—	—	—	—	—	—	512	30π	114	10^{-7}
E5	—	—	—	—	—	—	512	60π	234	10^{-7}

Analytical model

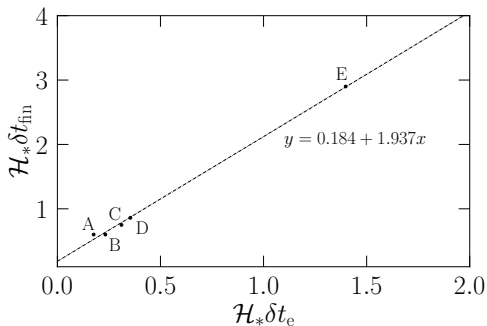
- Assumption: magnetic field evolution ($\delta t_e \sim 1/(v_A k_*)$) is slow compared to the GW dynamics ($\delta t_{\text{GW}} \sim 1/k$) at all $k \lesssim k_*$
- We can derive an analytical expression for the envelope over the oscillations¹⁴ of $\Omega_{\text{GW}}(k)$

$$\Omega_{\text{GW}}(k, t_{\text{fin}}) \approx 3 \left(\frac{k}{k_*} \right)^3 \Omega_{\text{M}}^*{}^2 \frac{\mathcal{C}(\alpha)}{\mathcal{A}^2(\alpha)} p_{\Pi} \left(\frac{k}{k_*} \right) \\ \times \begin{cases} \ln^2[1 + \mathcal{H}_* \delta t_{\text{fin}}] & \text{if } k \delta t_{\text{fin}} < 1, \\ \ln^2[1 + (k/\mathcal{H}_*)^{-1}] & \text{if } k \delta t_{\text{fin}} \geq 1. \end{cases}$$

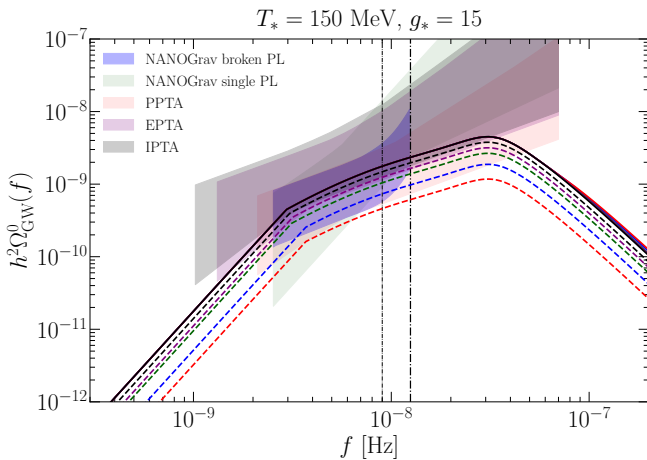
¹⁴ ARP et al., *Phys. Rev. D* **105**, 123502 (2022)

Analytical model

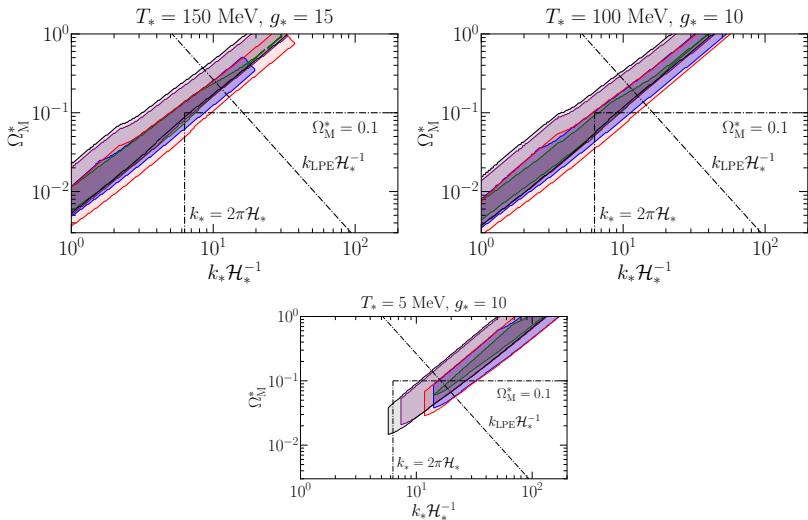
- The effective duration of the source t_{fin} that determines the position of the k^3 break is not given by the analytical model.
- We expect it to be a function of the eddy turnover time t_e
- From the simulations, we obtain the following empirical fit:



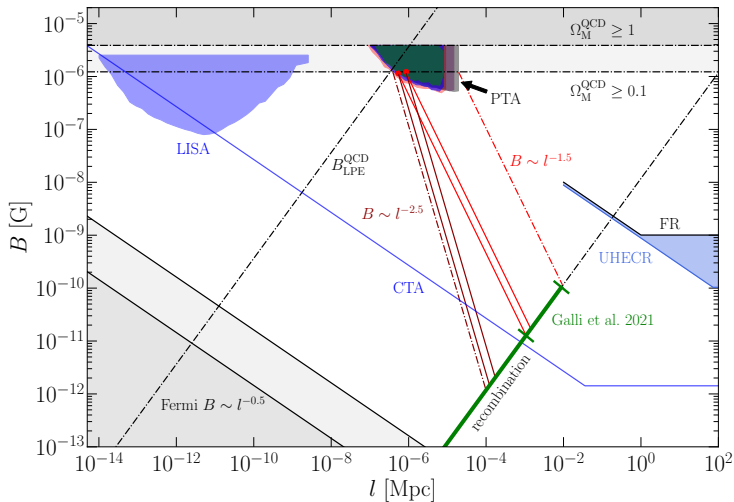
Using PTA to constrain the primordial magnetic field¹⁵



Using PTA to constrain the primordial magnetic field¹⁶



Using PTA (and LISA) to constrain the primordial magnetic field¹⁷



Conclusions

- We have performed simulations of MHD turbulence to study the stochastic GW background produced by primordial magnetic fields during the radiation-dominated era (e.g., at the scale of the QCD phase transition)
- The dynamical evolution of the magnetic fields is slow compared to the time scales of the SGWB production, which allows to assume constant magnetic stresses
- The analytical model derived works very well to predict the SGWB shape and amplitude, especially for magnetic fields with low eddy turnover times
- The SGWB presents a f^3 spectrum at low frequencies and a transition towards f below the spectral peak at $f_{\text{GW}} > f > 1/\delta t_{\text{fin}}$
- The effective duration of the source cannot be predicted from the analytical model, so we have used numerical simulations to obtain a fit as a function of the eddy turnover time
- We have constrained the parameters of the magnetic field using the analytical model compared to the observations from the PTA collaborations:
$$2 < T_*/\text{MeV} < 200, \quad \Omega_M^* > 0.01, \quad I_* > 0.1 \mathcal{H}_*$$
- The derived model has also been applied to LISA and it can be applied to other detectors, e.g., Einstein Telescope

The End Thank You!



roperpol@apc.in2p3.fr

github.com/AlbertoRoper/GW_turbulence
albertoroperpol.wixsite.com/roperpol